

Reservoir diagnosis of longwall gobs through drawdown tests and decline curve analyses of gob gas venthole productions

Heather N. Dougherty*, C. Özgen Karacan, Gerrit V.R. Goodman

NIOSH, Pittsburgh Research Laboratory
Pittsburgh, PA 15236

1. Introduction

During longwall mining, fracturing and relaxation in the gob creates new and highly permeable flow paths. Methane inflow from the gob into the mining environment is influenced by the magnitude of fracturing and the extent to which the fractures stay open during mining. Singh and Kendorski [1] evaluated the disturbance of rock strata resulting from mining and described a caved zone that extends from the mining level to 3 to 6 times the seam thickness, a fractured zone that extends from the mining level to 30 to 58 times the seam thickness, and a bending zone where there is no change in permeability that extends from 30 times the seam thickness to 50 ft below ground surface. The characteristics of fracturing and the subsidence of overburden were revealed through predictive techniques and field studies [2-6]. It was concluded that rock failure leading to increased hydraulic conductivity in the gob was initiated by high compressive stresses ahead of the face with the fractures subsequently opened by tensile stresses behind the face [7].

Gas, particularly methane that is contained within the gob, will be released over time as mining progresses and is a big contributor to ventilation emissions if not controlled. Relaxation of the roof rocks, ventilation pressure and the associated fracture connectivity allows gas to flow from all surrounding gas sources toward the mine workings, which eventually may create an unsafe condition for the underground workforce.

As longwall mining continually progresses, the caved zone in the gob gradually consolidates to support large loads resulting from the overburden weight [8]. This consolidation results in a reduction in the initial porosity and the associated permeability, where prevailing high permeability pathways in the consolidated gob still affect the flow

of methane from surrounding sources into the gob and into the mine. Thus, an understanding of resultant reservoir properties of gob material is very important for developing adequate methane control strategies [9].

One common technique to control methane emissions is to drill vertical gob gas ventholes (GGV) equipped with exhausters into each longwall panel to capture the methane within the overlying fractured strata before it enters the work environment. Gas production from GGVs may exhibit variable gas quality. In the early stages of production, the gas quality is generally high (> 80%) after a hole is intercepted by the longwall. Relatively high production rates with high methane quality are usually sustained for a few weeks. Later in time, especially towards the end of the panel mining or after the panel is completed, gob gas production may exhibit decreased methane levels as ventilation air is drawn from the active mine workings. When the methane concentration in the produced gas reaches 25%, the exhausters are commonly de-energized as a safety measure and the holes allowed to free flow.

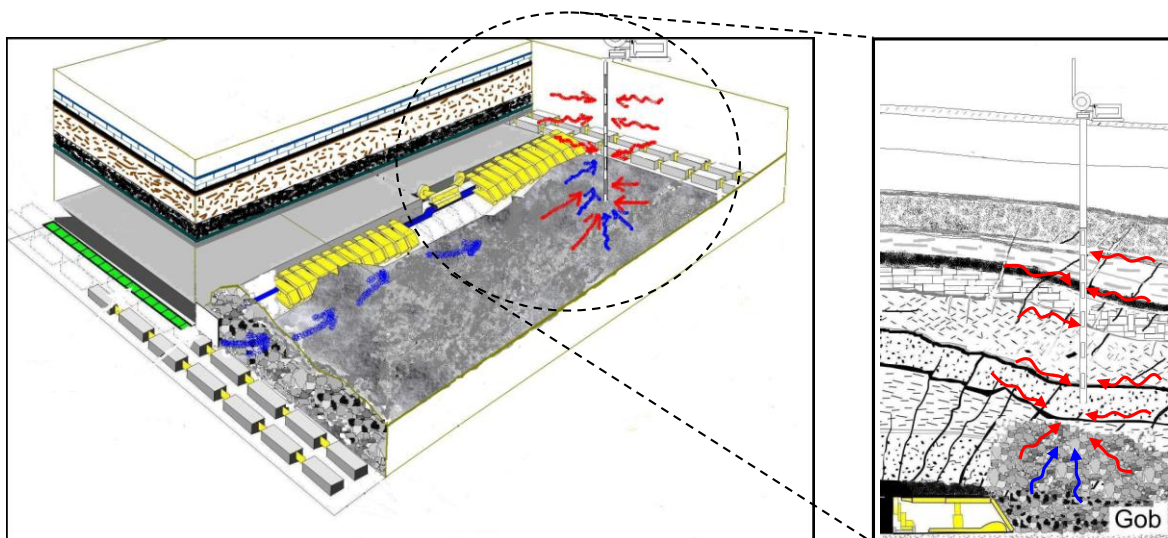


Figure 1. Schematic representation of a longwall and gas leakage and migration pathways to GGV in a gob environment.

Some of the barriers towards effective management of methane in mines through use of gob gas ventholes are the complexity of the gob environment, the involvement and interdependence of multiple influential factors, and the lack of knowledge on

interactions of the GGV with the gob reservoir. Improvements in venthole gas drainage evaluation and prediction capabilities for site-specific mining conditions and circumstances can address longwall gas emission issues, resulting in ventholes designed for improved gas capture. At this juncture, well test and production analyses methods, such as multi-rate drawdown [10] and decline curve analyses, which are applied in the petroleum and natural gas industry and in coalbed methane reservoirs, can be effective to understand the transport characteristics of the gob reservoir and to forecast production potential of gob gas ventholes.

In this paper, the production rate-pressure behavior of a gob gas venthole (GGV) drilled over a longwall panel was analyzed by using multi-rate drawdown and decline curve analysis techniques. The analyses were performed for a pseudo-steady state (PSS) flow period, which started when mining of the panel was complete and manifested itself with the production decrease from gob gas ventholes. In PSS, both drawdown and decline curve analyses could be carried out simultaneously [10]. Multi-rate production drawdown and decline curve analysis techniques were used to diagnose the properties of the gob reservoir and GGV such as skin, permeability, radius of investigation, flow efficiency, damage ratio and production decline rate of the venthole.

* Corresponding author. E-mail: iggq0@cdc.gov

2. Overburden stratigraphy in the study area and the location of study GGV

This study was conducted in the Northern Appalachian Basin in Southwestern Pennsylvania, Greene County, Pennsylvania. This area is very important for coal mining and for mining-related methane emissions and capture using conventional boreholes and gob gas ventholes.

In the study area, most of the longwall mining operations exist in the Pittsburgh seam of the Monongahela Group and the methane emissions from the gobs of these operations are captured using GGVs. The Monongahela Group is located within the Pennsylvanian age sediments and includes the interval from the base of the Pittsburgh coal to the top of the Waynesburg coal. The general coal measures in the Monongahela

Group in Greene County are limestones, sandstones and mostly shale and coal sequences of varying thicknesses. Markowski [11] reported that the main coal beds that are consistent and continuous in the study area are the Pittsburgh, Sewickley, and Waynesburg. The Redstone coal bed and Pittsburgh rider coals are not continuous and can be present at some locations. In this interval, the Sewickley coal bed, the gassy sandstones within the gob interval and the Redstone and rider coals are believed to be the main source of gob methane produced by GGVs.

Figure 2 shows an example stratigraphic plot of these layers using the data from a core-hole and the relative location of the slotted casing with respect to the geologic layers [6]. The example core log given in Figure 2 shows the average thickness of various formation layers. It also shows that there is a thick sandstone layer (sandstone paleochannel) above the Pittsburgh coal bed. However, this layer is not persistent in the study area and both its presence and its thickness change with location (Figure 3). When it exists, depending on its thickness, the bottoms of the slotted casings of the ventholes may be either in this sandstone or over it in a close proximity. The formation types and their thicknesses are characteristic of coal measure strata deposited in swamp and lacustrine environments [12]. In such an environment, fracturing and bedding plane separations are more probable within an interval between 40 ft-145 ft from the top of the coal bed. This interval contains thin limestones, sandstones and weaker strata, such as coalbeds and shales [6]. This eventually affects the formation of the gob reservoir, gas availability and production of GGVs.

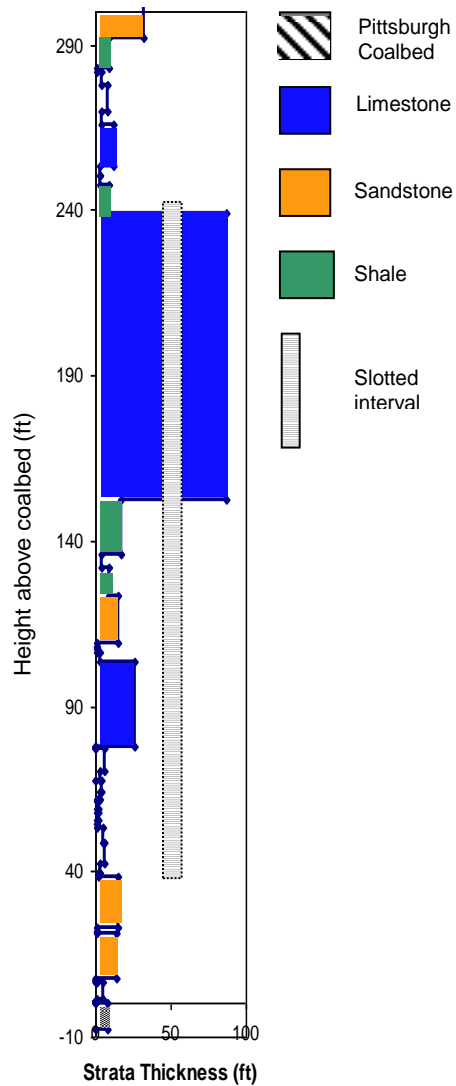


Figure 2. Stratigraphic representation of the overlying formations in the study area and the approximate location of the slotted casing interval (revised from [6]).

3. Completion and monitoring of the GGV for production and pressure

The location of the instrumented and monitored venthole relative to the mined panel is given in Figure 3. It was drilled at a terrain with 789.76 ft overburden to the mine and completed using 8-inch casing up to 45 ft from the top of the coal bed. The lower 200-ft of the venthole was completed with slotted casing for flow entry. The borehole was positioned 223 ft from the tailgate and 2132 ft from the start of a panel 10,798 ft in

length and 1225 ft in width. Figure 3 also shows the areas where the sandstone paleochannel exists in the study area and the variation of its thickness. Based on this map, the monitored GGV is located in an area where there was no sandstone on the top of the Pittsburgh coalbed.

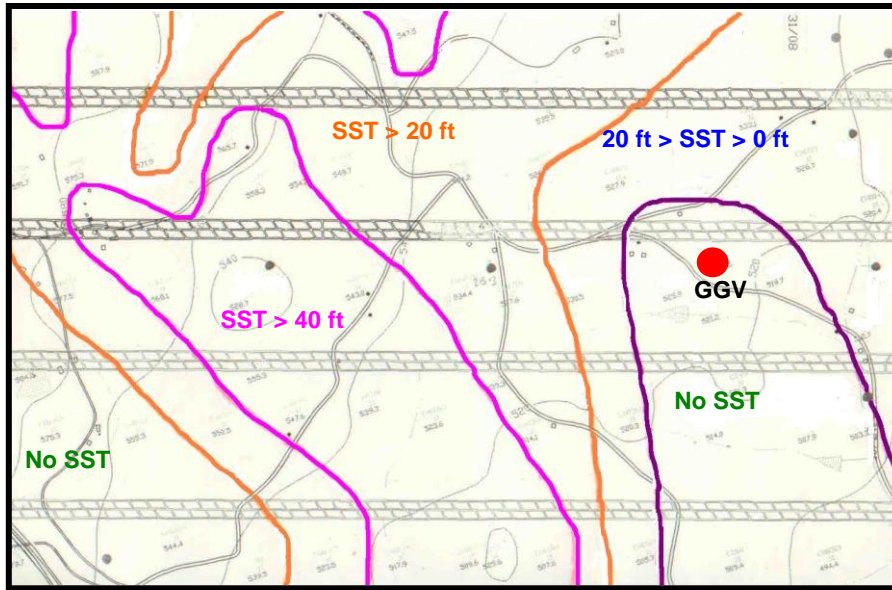


Figure 3. An areal representation of mined panels and the location of the monitored GGV. The drawing also shows the areas where the sandstone (SST) paleochannel exists and its thickness distribution. Mining direction in the panels is from right to left of the figure.

In order to analyze the pressure-production relationship of boreholes for their transient behaviors, the boreholes should be instrumented downhole to measure the flowing bottom-hole pressures and the flow rates. Since the operation of the gob gas ventholes is closely related to the underground safety of the miners, maintaining intrinsic electrical safety is a must with any instrumentation used downhole to prevent possibility of an accident. To avoid these risks, the study venthole was instrumented on the surface ahead of the exhauster to measure the total flow rate, methane percentage, temperature and pressure at the wellhead.

The pressure and production behaviors of the venthole were monitored throughout the mining of the panel and after panel completion. In this study, only the data acquired after completion of the panel were analyzed since this period is close to a pseudo-steady state flow regime where both multi-rate drawdown and decline curve analysis techniques can be used.

The total gas production in gob gas ventholes comes from different sources at different depths of the slotted casing interval and is produced as a mixed gas stream by a methane-driven exhauster that provides vacuum at the wellhead. Thus, it is important to know the reservoir and fracturing characteristics of the formations in which the slotted casing is located.

Figure 4 shows the total gas production and wellhead pressure history of the monitored gob gas venthole after completion of panel. The production times in this figure are the elapsed times after the completion of the respective panel. Although the data is scattered, the general trends in observed gas productions show that the venthole produced at higher gas rates just after completion of the panel and that the rates entered a decline period with increasing time. Also, comparison of the data in Figure 4 show that total gas production rate does not necessarily correlate with applied vacuum (wellhead pressure). Although a vacuum applied to the gob gas ventholes stimulates methane migration into the ventholes from the surrounding strata and prevents occasional flow reversals [13], this advantage may be lost over time as there is tendency for mine air to be drawn into the gob area, diluting the methane [14]. A higher suction pressure has a positive but relatively small effect on drawing gas from overlying strata into the venthole. In the monitored venthole, the wellhead vacuum pressures were generally between 12.0-12.8 psia (Figure 4) and the wellhead pressures tended to increase (less suction) over time after the panels were completed due to a lower methane flow rate. Pressure data at the wellhead that is presented in Figure 4 had a mean value of 12.52 psia with 0.2 standard deviation. The recorded minimums and maximums were 12.02 psia and 12.82 psia, respectively. On the other hand, declining gas production data had a minimum and maximum recorded value of 0.3046 MMscf/day and 0.6311 MMscf/day, respectively. The mean and standard deviation of this data were 0.4425 MMscf/day and 0.0978, respectively, during the monitoring period.

Figure 5 shows the methane concentration in the total gas production of monitored gob gas venthole after completion of the panel. The data show that the venthole initially produced with ~50% methane. However, after the wellhead vacuum decreased at about 800 hrs, methane concentration increased to ~60%.

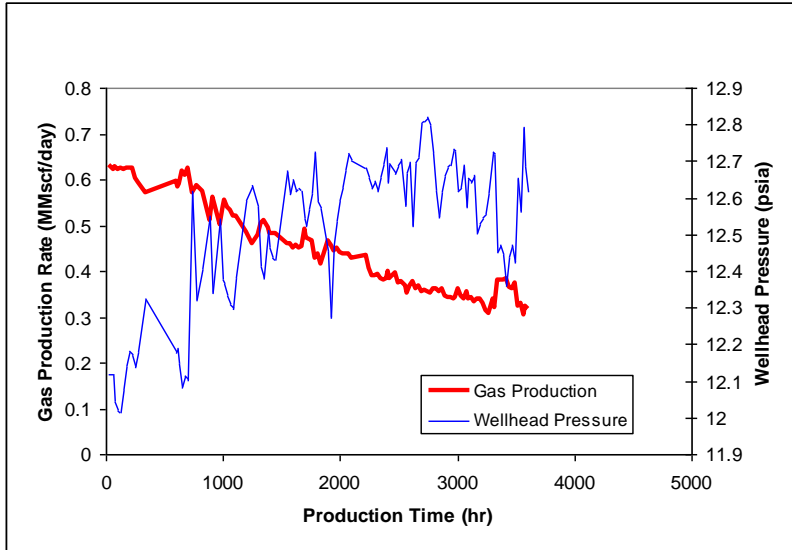


Figure 4. Gas production rate and wellhead pressures measured from the monitored GGV as a function of time after the completion of the longwall panel.

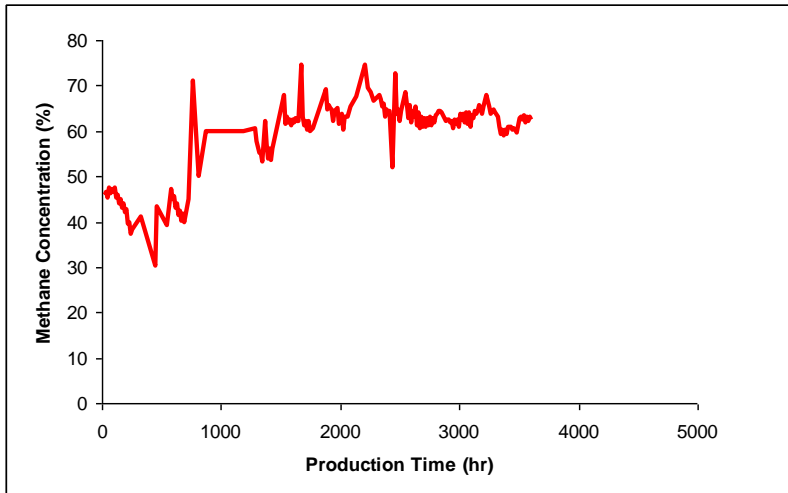


Figure 5. Methane concentration measured from the monitored GGV as a function of time after the completion of the longwall panel.

4. Production-pressure test and data analyses techniques

Routine production tests that are performed in the oil and gas industry are usually expensive and require sophisticated downhole instrumentation and analysis methods developed by various researchers [15-17]. For unconventional wells such as GGVs, the development of specific testing and interpretation methods remained nonexistent due to various complexities related to the gob reservoir and shorter production lives of gob gas ventholes compared to conventional boreholes. However, the importance of understanding the properties of the gob reservoir still remains a critical issue in controlling methane in the mining environment. This study presents application of conventional gas-well testing methods for analyzing GGV productions from longwall gob reservoirs.

4.1. Multi-rate drawdown test and analysis

In order to evaluate production and pressure data obtained from the monitored gob gas venthole, a multi-rate drawdown analysis was carried out using a commercial well test analysis software. In this study, a two-zone composite radial model with a vertical borehole was used for a pseudo-steady state (PSS) flow period in the after-panel-completion production phase of the venthole [10]. The composite model assumes that the reservoir properties change at a certain radius from the borehole. For a gob reservoir, this assumption can be considered as a valid one since the properties of gob change in the cross-panel direction due to subsidence and compaction. Thus, there may be a different flow-capacity (kh) reservoir around the borehole to some distance into the gob in the radial direction, as compared to the rest of the gob reservoir.

The basic mathematical theory behind this test and the constant rate solution for analyzing pseudo-steady state flow regime can be given as [18]:

$$\psi_{wf} = \psi_i - 1.417 \times 10^6 \frac{q_g T}{kh} \left[\frac{0.000527 k t_a}{\phi \mu_{gi} c_{ii} r_e^2} + \ln\left(\frac{r_e}{r_w}\right) - \frac{3}{4} + s' \right] \quad (1)$$

In this equation, the following variables are used: ψ – pseudo-pressure for gas in psi^2/cp , q – gas flow rate in scf/d , k – permeability in md , h – net pay in feet, Φ – porosity, μ – gas viscosity in cp , r_e – radius of investigation of the borehole in feet, s' – total skin factor, c_{ti} – the total compressibility and q – flow rate. The subscripts used are w – wellbore, f – flowing, i – initial, and g – gas.

This equation is linear with time and, thus, pseudo-steady state (PSS) flow data forms a straight line when plotted on a Cartesian plot. From this equation, parameters such as k , r_e and s' , can be determined by using calculated pseudo flow rate, time (t) and temperature (T) at the downhole, or wellhead. Also, the derivative analysis can be carried out by taking the derivative of equation (1) with respect to time. This result is linear with time and the derivative of PSS data on a log-log plot is a straight line with unit slope.

Thus, when $\log(\frac{\Delta\psi}{q})$ versus $\log(t_{\text{PSS}})$ is plotted, the plot shows a straight line or a straight-line trend.

However, in order to apply above techniques for multi-rate production histories, the “elapsed time” should be defined in terms of superposition time. Superposition in time for a well producing with multiple rate conditions for various durations means that individual constant rate wells can be placed in the same position in the reservoir at any time [18]. The superposition time used in this study to analyze the data was:

$$t_n = \sum_{j=1}^n \frac{q_j - q_{j-1}}{q_n} \log(t - t_{j-1}) \quad (2)$$

Using PSS multi-rate drawdown well test analyses techniques briefly presented here, flow efficiency (FE) of a well can be calculated. FE is a relative index that is defined as the ratio of the actual productivity index of a well to its productivity when there is no skin ($s' = 0$). Skin is the additional pressure drop because of reduction in permeability near the well due to factors in the drilling and completing processes. Flow efficiencies of about 2.0 may be obtained after hydraulic fracturing in formations of moderately high permeability; in low permeability formations, the FE may reach 5.0 after

a fracture treatment [19]. The relationship that was used in this study to calculate flow efficiency is:

$$FE = \frac{\bar{\psi} - \psi_{wf0}}{\bar{\psi} - \psi_{wf0} - 0.869 m s'} \quad (3)$$

where m is the slope of the transient plots

Similarly, the damage ratio (DR), which is also a relevant index, was calculated by taking the inverse of flow efficiency. Thus, higher FE and lower DR indicate better reservoir-flow properties and more productive boreholes.

4.2. Traditional decline curve test and analysis

Traditional decline curve analysis is a graphical procedure used for analyzing declining production rates and forecasting future performance of wells. A curve fit of past production performance is done, which then is extrapolated to predict potential future performance by identifying the type of the decline based on historical observations of well performance. Empirically, three types of decline curves have been identified; exponential, hyperbolic, and harmonic. There are theoretical equivalents to these decline curves. For instance, under constant producing wellbore pressure and pseudo-steady state conditions, equations of fluid flow through porous media are equivalent to an exponential decline, which also was used in this study.

When analyzing rate decline, two sets of curves are plotted using the production data. The flow rate is plotted against either time or cumulative production. Under ideal conditions, plots of log-rate vs. time and rate vs. cumulative production should both result in straight lines from which the decline rate can be determined. This decline is called constant rate or constant percentage decline, which is observed in exponential decline.

In decline curve analysis, it is implicitly assumed that the factors causing the historical decline continue unchanged during the forecast period. These factors include both reservoir conditions and operating conditions of the borehole. As long as these conditions do not change, the trend in decline can be analyzed and extrapolated to forecast future well performance. This implicit assumption is especially valid for gob

reservoirs after completion of the panel since caving and subsidence are complete at this stage and no major reservoir changes are expected.

All traditional decline curve theory starts from the definition of the current decline rate (D) as:

$$D = -\frac{(\Delta q/q)}{\Delta t} = \frac{(\Delta q)}{\Delta t} / q \quad (4)$$

For exponential decline, D is the decline rate and it is a constant.

$$\frac{q}{q_i} = \frac{1}{e^{Dt}} \quad (5)$$

$$\text{or, } \log\left(\frac{q}{q_i}\right) = -\frac{Dt}{2.303} \quad (6)$$

These equations show that a plot of log-rate versus time will yield a straight line of slope D/2.303. Cumulative production (Q) can be obtained by integrating the rate-time relationship and is shown as:

$$q = q_i - DQ \quad (7)$$

Equation 7 results in a plot of rate versus cumulative production with a constant slope D and can be extended to any abandonment rate to obtain the recoverable reserves.

5. Results and discussion

A multi-rate production drawdown test in a PSS flow regime was initially used to determine average reservoir parameters and the total skin around the venthole. This model predicted that the end of mining and sealing of the panel would create a bounded reservoir effect on the venthole's production in which the pressure transients reach the outer boundaries very quickly and start a pseudo-steady state flow period. According to this concept, a two-layer composite model that defined the reservoir heterogeneity as

around-the-borehole (Zone 1) and far-from-the-borehole (Zone 2) zones was created and the analyses were carried out based on this model (Figure 6). The composite model assumes that the reservoir properties change at a certain radius from the borehole. This phenomenon does not necessarily occur in nature, although some reservoirs behave like they are composite. For instance, a borehole drilled in a naturally fractured reservoir with different fracture distributions around the well path may behave as composite reservoir. For a gob reservoir, this assumption can be considered as a valid one since the properties of the gob change in the cross-panel direction due to subsidence and compaction. Consequently, there may be a different flow capacity (kh) reservoir around the borehole to some distance into the gob in the radial direction, as compared to the rest of the gob reservoir.

It is also important to state that the model used in this study considers the gob as a homogeneous and single porosity structure despite the fact that there are various heterogeneities in the gob, including fractures, bedding plane separations, and tension and compression zones. Even for conventional oil and gas reservoirs that do not experience major strata disturbances, there is not a single reservoir that is actually homogeneous. However, it has been suggested that many reservoirs behave homogeneously during production and well test analyses. Therefore, in the absence of the information on the exact heterogeneities and their locations, the homogeneous model assumption is the most widely accepted one in well test analysis [20].

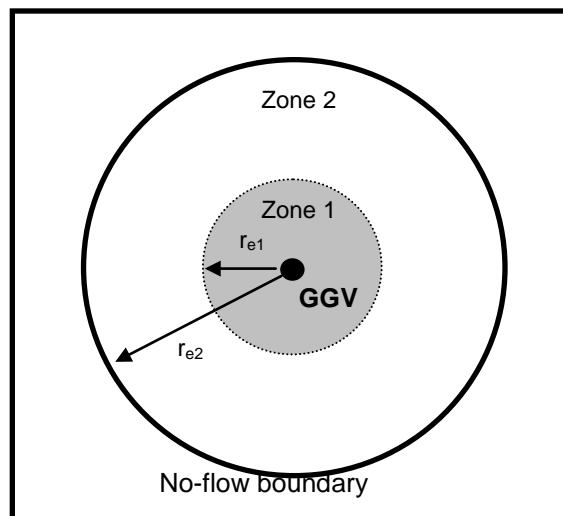


Figure 6. Schematic representation for the composite model of gob where PSS flow occurs around the GGV.

The calculated data and the model predictions for wellhead pressure histories on linear scale (B-plots), linear superposition PSS time versus $\frac{\Delta\psi}{q}$ (A-plots) and log-log scale (C-plots) are presented in Figure 5. Monitored and model data are given in the same plots for comparison purposes. These figures show that the model predictions using linear, and log-log data and derivatives are generally good for the data obtained from venthole production and pressures. By using the data of these plots, average reservoir parameters and wellbore skin parameters were calculated for the monitored venthole. The results of these analyses for the PSS flow regime of the venthole are given in Table 1. During the analyses, the radius of each zone in this composite model was determined using an APE (Automatic Parameter Estimation) algorithm, as well as their reservoir properties.

Table 1. Results of gob properties calculated using multi rate drawdown analysis

| Parameter | Value |
|-----------------------------|---------|
| r_{e1} (ft) – first zone | 360.8 |
| k_{re1} (md) | 524.1 |
| r_{e2} (ft) – second zone | 9173.8 |
| k_{re2} (md) | 15648.5 |
| Total skin (s') | -6.1 |
| Final rate (MMscf/day) | 0.317 |
| Cum. prod. (MMscf) | 68.803 |
| Final flow pressure (psia) | 12.6 |
| Ave. error (%) | 0.70 |
| FE | 8.2 |
| DR | 0.1 |

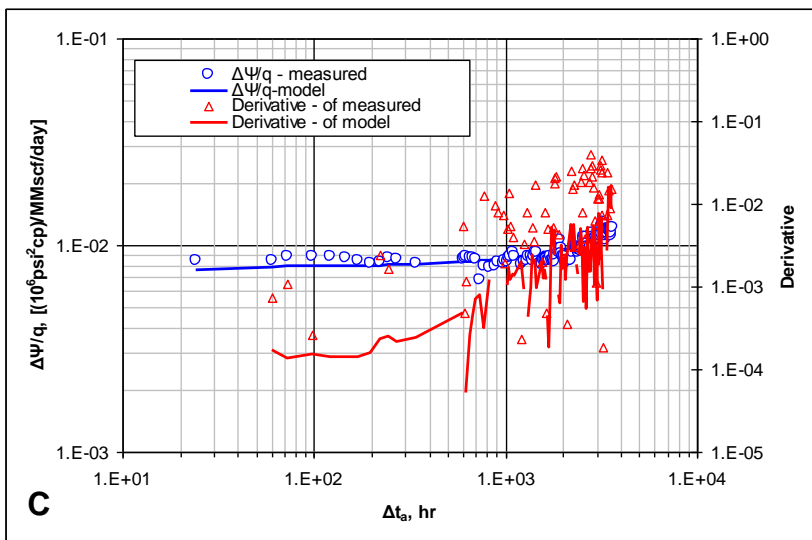
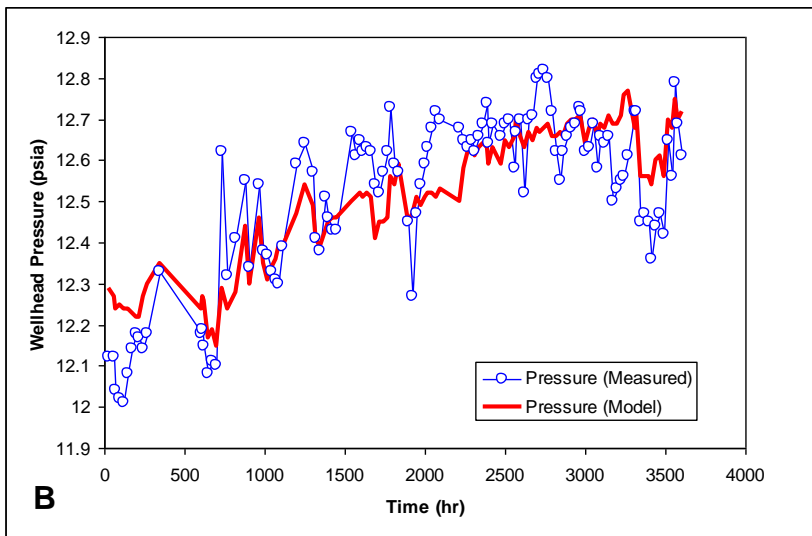
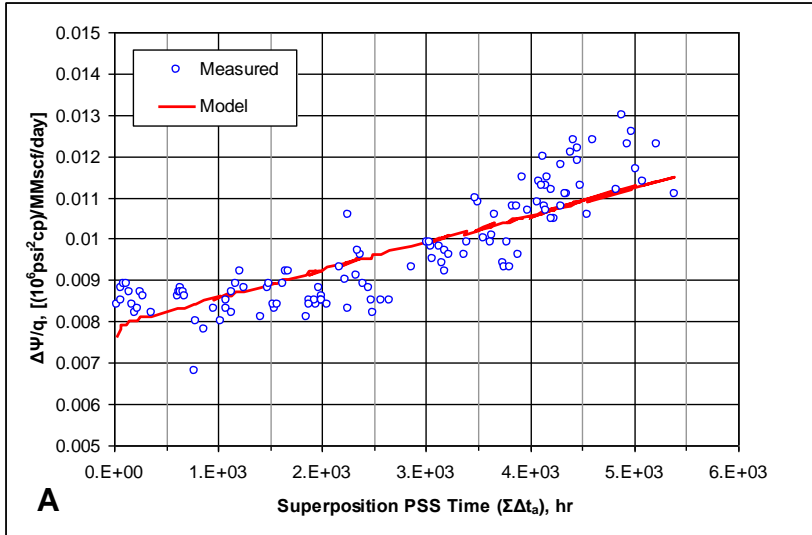


Figure 7. Plots of superposition time (A), linear wellhead pressure match showing measured and the model pressure (B) and log-log flow potential and derivative (C) for analysis of a gob gas venthole using the multi rate drawdown technique in a radial pseudo-steady state acting period in a closed reservoir (after mining).

Table 1 presents the findings of permeability and radius of investigation results in the first four rows. However, it should be kept in mind that these average effective permeabilities were calculated for the whole 200 ft section open to flow through the casing slots using a homogeneous model. Thus, individual fractures or bedding plane separations might have higher permeabilities in various areas in the 200 ft section.

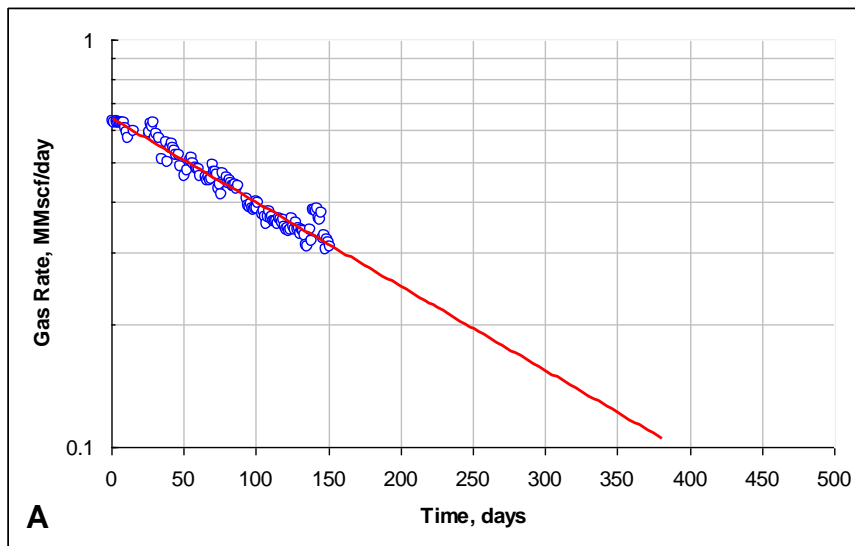
Also, it should be emphasized that, although the radius of investigation is frequently viewed as the minimum radial distance to any event that may not be observed during the test period, the transient radius may be greater than the radius of investigation estimated from well tests due to layer permeability and saturation variations. This is certainly a valid observation for the current study due to the known existence of fractures and bedding layer separations during mining. Thus, due to the averaging effects of the interpretation results, the complete reservoir area affected by the well production may be confined in a different circular area around the wellbore [21]. The calculated radius of investigation from the well test gives an approximate value and an order of magnitude idea about the true distance for the existence of boundaries [19] rather than an exact distance.

Table 1 shows that the calculated permeabilities were highest in the second radial zone in this venthole. The permeability of this zone was calculated as ~15650 millidarcies (md) extending to a radius of about 9200 ft from the venthole location. The permeability in the immediate vicinity of the venthole (first radial zone) was about 525 md and with a radius of 360 ft. The calculated total skin around the venthole was -6.1. Thus, due to fracturing of the overlying formations of the gob as a result of mining, the venthole actually behaves like a fracture-stimulated borehole. This venthole also had the highest flow efficiency (8.2), which resulted in high methane production, cumulative gas production (68.8 MMscf), and high production rates. The total gas production rates were

0.63 MMscf/day at the start of decline and 0.317 MMscf/day at the end of the production duration at 3600 hours after the panel was completed (Figure 4 and Table 1).

A traditional decline curve analysis was also performed for the data obtained from this venthole. The log-rate versus time (A) and rate versus cumulative production (B) plots are given in Figure 8. These plots show that the production rate behavior resulted in straight lines. Thus, the decline rates for this venthole after panel completion are essentially exponential during the monitoring period (3600 hrs).

Analysis of Figure 8-A and Figure 8-B results in a constant decline rate of 0.0048 /day for this venthole and indicates an expected ultimate recovery (E.U.R) of 90 MMscf of gas at an abandonment rate of , for example, 50 Mscf/day (34 scfm). The abandonment rate is the rate at which the well is no longer economically feasible. Approximately 69 MMscf of gas was already produced (Table 1) by the end of 151 days (3600 hours) of production and about 21 MMscf could still to be produced. However, the recoverable methane will be much less since the methane percentage is around 60% and will continue to decrease. It will also take the venthole about 2.7 years to reach this abandonment rate. Table 2 gives the results of exponential decline curve analysis.



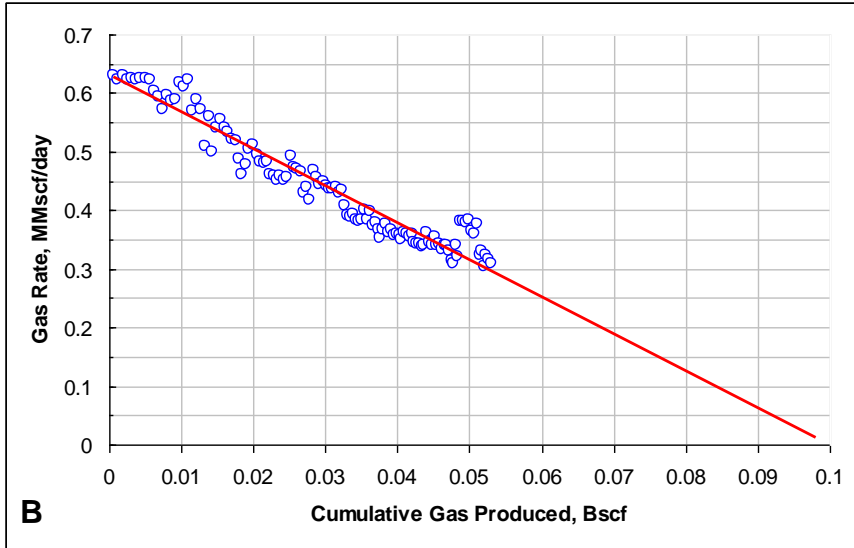


Figure 8. Exponential – constant rate – decline curve analysis. Plots of rate (log) versus time (A) and rate versus cumulative production (B).

Table 2. Results of exponential decline curve analysis for the analyzed GGV. Bscf – Billion scf

| Decline Relations | |
|----------------------|---|
| Rate-Cum. Production | Rate (MMscf/day) = -6.3194 × (Cum. Prod. – Bscf) + 0.6304 |
| Rate (log) – Time | Rate (MMscf/day) = 0.6421e-0.0048 × (Time-days) |

6. Conclusions

In this study, conventional well-test techniques are suggested as a promising way to evaluate complex gob reservoirs and to assess gob gas venthole performance. However, the results and the interpretations showed that the well test results should be evaluated with the integration of local geological and geophysical data, as commonly practiced in the oil and gas industry.

The results suggest that conventional well-test analyses and GGV production behaviors after mining of a longwall panel can be used determine important parameters. These parameters are wellbore skin, permeability, radius of investigation, flow efficiency,

damage ratio and percentage decline, which help in production forecasting and evaluating project economics. The insights obtained from well test analyses can also be used for a better understanding of the gob and for designing more effective gob gas venthole systems for methane control in longwall mines.

The specific results obtained from this borehole using a PSS radial flow approach for gob reservoirs indicated that the reservoir permeabilities can be as high as 15.6 darcies, skin values as low as -6, and flow efficiencies as high as 8.2. These parameters corroborate the high productivity of gob gas ventholes in this highly fractured and permeable environment.

Finally, it is worthwhile to mention about some of the limitations associated with application of conventional well test techniques to rate and pressure analyses of GGVs. Some of these limitations are direct consequences of the assumptions that are also mentioned in this application study. For instance, radial flow regime was assumed in the gob reservoir that had no-flow upper and lower boundaries. This assumption was justified due to the fact that the slotted section of the venthole spanned almost entirety of the methane emission sources. However, this may not always be the case due to extensive fracturing and due to the possibility of bedding plane separations, which result in development of linear channel flow toward the borehole rather than radial flow. Also, interferences may not be neglected all the time and a multi-well analysis should be conducted with the pressure and reservoir data. Complexity of the gob and structural heterogeneity may also create major limitations to application of well-test techniques since most oil and gas reservoirs do not have the same degree of heterogeneity that is captured by theoretical equations. This situation can be eased by averaging, if and when possible, the heterogeneities to scale them down to a homogeneous model, as presented in this paper.

References

- [1] Singh, M.M., Kendorski, F.S. Strata disturbance prediction for mining beneath surface waters and waste impoundments. In: proceedings of 1st International Conference on Ground Control in Mining, Morgantown, WV, 1981, p76-89.

- [2] Li, S., Lin, H., Cheng, L., Wang, X. Studies on distribution pattern of and methane migration mechanism in the mining-induced fracture zones in overburden strata. In: proceedings of 24th International Conference on Ground Control in Mining, Morgantown, WV, 2005, 268-273.
- [3] Cui, X., Wang, J., Liu, Y. Prediction of progressive surface subsidence above longwall coal mining using a time function. *International Journal of Rock Mechanics and Mining Sciences* 2001;38:1057-1063.
- [4] Luo, Y. An integrated computer model for predicting surface subsidence due to underground coal mining (CISPM). PhD dissertation, Department of Mining Engineering, West Virginia University, Morgantown, WV. 1989.
- [5] Palchik, V. Localization of mining-induced horizontal fractures along rock layer interfaces in overburden: field measurements and prediction. *Environmental Geology* 2005;48: 68-80.
- [6] Karacan, C.Ö., Goodman, G.V.R. Hydraulic conductivity and influencing factors in longwall overburden determined by using slug tests in gob gas ventholes, *International Journal of Rock Mechanics and Mining Sciences* 2009; 46: 1162-1174
- [7] Liu, J., Elsworth, D. Three-dimensional effects of hydraulic conductivity enhancement and desaturation around mine panels. *International Journal of Rock Mechanics and Mining Sciences* 1997;34:1139-1152.
- [8] Pappas, D.M., Mark, C. Behavior of simulated longwall gob material. Report of Investigations No. 9458, US Dept. of Interior, US Bureau of Mines. 1993, 39 pp.
- [9] Karacan, C.Ö. Prediction of porosity and permeability of caved zone in longwall gobs. *Transport in Porous Media* 2010; 82: 413-439.
- [10] Karacan, C.Ö. Reconciling longwall gob gas venthole performances using multiple-rate drawdown well test analysis, *International Journal of Coal Geology* 2009; 80: 181-195.
- [11] Markowski, A. Coalbed methane resource potential and current prospect in Pennsylvania. *International Journal of Coal Geology* 1998;38:137-159.
- [12] Karacan, C.Ö. Reservoir rock properties of coal measure strata of the Lower Monongahela Group, Greene County (Southwestern Pennsylvania), from methane

- control and production perspectives. *International Journal of Coal Geology* 2009;78: 47-64.
- [13] Thakur, P.C. Coal seam degasification. In: Kissell, F. (Ed.) *Handbook for Methane Control in Mining*, National Institute for Occupational Safety and Health Information Circular No: 9486, Pittsburgh, PA, 2006, 77-96.
- [14] Ren, T.X., Edwards, J.S. Goaf gas modeling techniques to maximize methane capture from surface gob wells. In: *Mine Ventilation*, Euler De Souza (Ed.). 2002, 279-286.
- [15] Kuchuk, F.J., Onur, M., Estimating permeability distribution from 3D interval pressure transient tests. *Journal of Petroleum Science and Engineering* 39:5-27.
- [16] Valvatne, P.H., Serve, J., Durlofsky, L.J., Aziz, K. Efficient modeling of nonconventional wells with downhole inflow control devices. *Journal of Petroleum Science and Engineering* 2003;39:99-116.
- [17] Escobar, F.H., Ibagón, O.E., Montealegre-M., M. Average reservoir pressure determination for homogeneous and naturally fractured formations from multi-rate testing with the TDS technique. *Journal of Petroleum Science and Engineering* 99: 204-212.
- [18] Dake, L.P. *Fundamentals of Reservoir Engineering*. Elsevier, Amsterdam. 1978, 443 pp.
- [19] Matthews, C.S., Russell, D.G. *Pressure Buildup and Flow Tests in Wells*. Society of Petroleum Engineers of AIME, Dallas, TX. 1967; 172 pp.
- [20] Bourdet, D. Practical aspects of well-test interpretation. In: Cubitt, J. (Ed.) *Handbook of Petroleum Exploration and Production*. Elsevier, Amsterdam. 2003, pp. 351-375.
- [21] Oliver, D.S. The averaging process in permeability estimation from well-test data. *SPE Formation Evaluation*, Sept., 1990, 319-324.